

---

---

**SEMICONDUCTOR STRUCTURES, INTERFACES,  
AND SURFACES**

---

---

## **Mechanism of Dislocation-Governed Charge Transport in Schottky Diodes Based on Gallium Nitride**

**A. E. Belyaev<sup>a</sup>, N. S. Boltovets<sup>b</sup>, V. N. Ivanov<sup>b</sup>, V. P. Klad'ko<sup>a</sup>, R. V. Konakova<sup>a</sup>, Ya. Ya. Kudrik<sup>a</sup>,  
A. V. Kuchuk<sup>a</sup>, V. V. Milenin<sup>a</sup>, Yu. N. Sveshnikov<sup>c</sup>, and V. N. Sheremet<sup>a</sup>**

<sup>a</sup>*Lashkarev Institute of Semiconductor Physics, National Academy of Sciences of Ukraine, pr. Nauki 45, Kiev, 03028 Ukraine*

<sup>e-mail</sup>: konakova@isp.kiev.ua

<sup>b</sup>*State Enterprise Research Institute Orion, ul. É. Pot'e 8A, Kiev, 03057 Ukraine*

<sup>c</sup>*ZAO Élma-Malakhit, Zelenograd, Moscow, 124460 Russia*

Submitted September 12, 2007; accepted for publication November 15, 2007

**Abstract**—A mechanism of charge transport in Au–TiB<sub>x</sub>–*n*–GaN Schottky diodes with a space charge region considerably exceeding the de Broglie wavelength in GaN is studied. Analysis of temperature dependences of current–voltage (*I*–*V*) characteristics of forward-biased Schottky barriers showed that, in the temperature range 80–380 K, the charge transport is performed by tunneling along dislocations intersecting the space charge region. Estimation of dislocation density  $\rho$  by the *I*–*V* characteristics, in accordance with a model of tunneling along the dislocation line, gives the value  $\rho \approx 1.7 \times 10^7 \text{ cm}^{-2}$ , which is close in magnitude to the dislocation density measured by X-ray diffractometry.

PACS numbers: 73.23.-b, 73.40.Sx, 73.40.Gk, 73.43.Jn

DOI: 10.1134/S1063782608060092

### 1. INTRODUCTION

In recent years, interest of developers of microwave devices to wide-gap semiconductor compounds of the III–N group has considerably increased. The interest is caused by real possibility of developing the devices for problems of extreme electronics. Gallium nitride is the most advanced in this respect. Its electrical characteristics are optimal for the development of thermally stable and radiation-resistant microwave diodes and transistors [1, 2]. However, with all the advantages of GaN, a disadvantage is the absence of a proper (gallium nitride) substrate material with area sufficient for mass production. Therefore, epitaxy of GaN on foreign substrates is accompanied by introduction of a considerable dislocation density in the growing film, prevalently misfit dislocations [3, 4]. In some studies performed for the III–V heterojunctions, Evstropov et al. showed that current flow in them, despite the fact that the heteropair is formed by nondegenerate semiconductors, is prevalently governed by multistep tunneling with involvement of dislocations even at room temperature [5–8]. For GaN, similar studies practically were not carried out.

The purpose of our study is to investigate the mechanism of the charge transport in the forward-biased Schottky diode based on the *n*–GaN–*i*–Al<sub>2</sub>O<sub>3</sub> heterostructure with a high dislocation density in *n*–GaN in a wide temperature range (80–600 K).

### 2. EXPERIMENTAL

In this paper, we report the results of studying the Au–TiB<sub>x</sub>–*n*–GaN Schottky diodes. Epitaxial *n*–GaN layers of  $\sim 1 \mu\text{m}$  thick with the concentration of donor impurity of  $\sim (1\text{--}3) \times 10^{17} \text{ cm}^{-3}$  were grown at ZAO Élma–Malakhit (Russia). Using the method of metal–organic vapor-phase epitaxy, we initially grew a heavily doped *n*<sup>+</sup>–GaN buffer layer on single-crystal Al<sub>2</sub>O<sub>3</sub> (0001) substrates, and then *n*–GaN layer was grown on the buffer layer. Structural quality of the *n*–GaN layers was studied by X-ray diffractometry. Ohmic contacts were fabricated based on the Au–TiB<sub>x</sub>–Al–Ti–*n*<sup>+</sup>–GaN metallization. The Au–Ti metallization was formed on the semi-insulating sapphire substrate with the purpose to mount the diode structure in the case. A chip of the diode structure is shown in Fig. 1a. Thicknesses of the layers were as follows: for the barrier contact Au (3000 nm)–TiB<sub>x</sub> (100 nm); for ohmic contact Au (2500 nm)–TiB<sub>x</sub> (100 nm)–Al (500 nm)–Ti (50 nm); and for metallization of sapphire Au (3000 nm)–Ti (50 nm). Distribution of components in contact metallization was studied by the Auger electron spectrometry. We described the physicochemical properties of contact systems with the TiB<sub>x</sub> diffusion barrier in [9]. Diode chips of 100  $\mu\text{m}$  in diameter were fabricated as direct mesa structures with the use of plasmochemical etching. To study mechanisms of charge transport, diode chips were mounted into the case (Fig. 1b), and forward portions of current–voltage (*I*–*V*) characteristics of the Schottky diodes were measured in a temper-

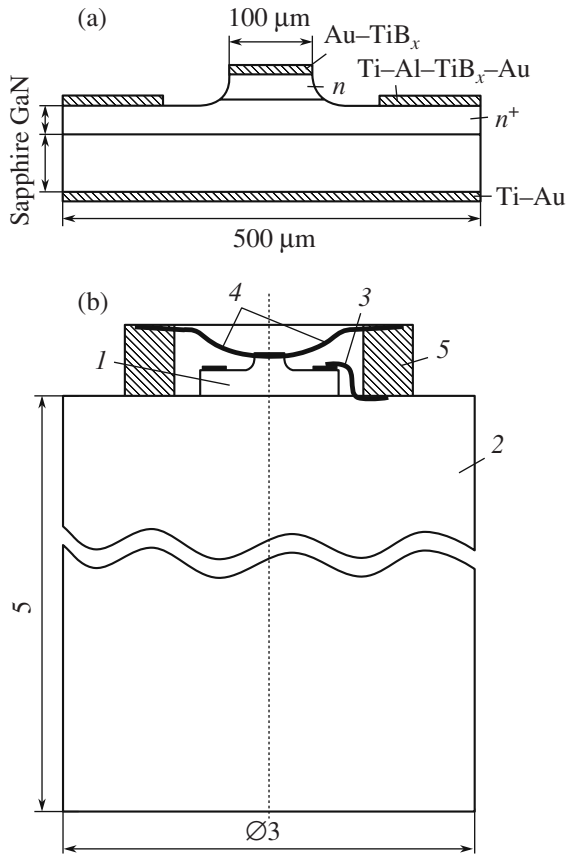


**Fig. 1.** (a) Chip of the diode structure and (b) design of the Schottky barrier in a metal-ruby case. Chip (1) is mounted onto copper golden-plated holder (2) by diffusion welding. The ohmic contact to the  $n^+$  layer is connected to the holder by thermal compression with the help of output wire (3). Then, a bushing with a metallized end is mounted onto the holder by diffusion welding. The upper electrode of the mesa-structure is connected to the end of ruby bushing (5) using the output wire (4).

ature range of 80–600 K. Capacitance–voltage ( $C$ – $V$ ) characteristics of the Schottky diodes were measured at 300 K. The main parameters of the Schottky diodes were calculated from experimental  $I$ – $V$  and  $C$ – $V$  characteristics.

### 3. RESULTS

Structural quality (dislocation density) of the samples was investigated by methods of high-resolution diffractometry via analysis of patterns of intensity distribution around the sites of the reciprocal lattice [4]. The used experimental schemes allow us to obtain two sections of the sites of the reciprocal lattice, namely, at a right angle to the diffraction vector ( $\omega$  scanning) and in parallel to the diffraction vector ( $\omega/2\theta$  scanning). Dislocation networks localized at the heterointerface cause the emergence of nonzero components of average distortion  $U_{xx}$  (obligatory) and  $U_{xz}$  (possibly) and broadening of the diffraction pattern along the perpen-

dicular to the vector of the reciprocal lattice irrespective of the direction of the latter.

Inclined spreading dislocations lead to broadening of the X-ray reflection both in the transverse direction and in the longitudinal direction with respect to direction  $\mathbf{H}$ , and the former is considerably larger. Inclusion-type defects lead to the emergence of diffuse scattering blurred around the site of the reciprocal lattice with the conservation (to some extent) of coherent scattering narrow-directed along the perpendicular to the surface of coherent scattering.

Two-dimensional diffraction patterns for the structures obtained in a three-axial experimental configuration are shown in Fig. 2. Here, we present the intensity distribution near the sites of the reciprocal lattice, symmetric (0004) (Fig. 2a) and asymmetric ( $-1-124$ ) (Fig. 2b). It follows from Fig. 2 that, in both cases, intensity distributions are elongated in the direction perpendicular to the  $\mathbf{H}$  vector.

Such behavior of intensity distribution is characteristic of a nonrelaxed sample with misfit dislocations. It is evident that the effect of dislocation networks on the Bragg diffraction amounts to broadening of the diffraction pattern in the direction perpendicular to the diffraction vector. The degree of this broadening (mosaicity) was determined by measurement of  $\omega$  scans, which fix the variation in intensity in this direction.

A characteristic feature of the diffraction pattern from epitaxial structures with dislocation networks is the absence of any noticeable intensity along the axis  $q_{\mathbf{H}}$ , where coherent scattering from perfect regions of the crystal should be localized. Dislocation networks in these structures are arranged at the heterointerface. Consequently, elastic fields of the dislocation network, which are the cause of the broadened diffraction reflection, are not localized near it but are rather far extended right up to the film surface.

Measurements were performed using a PANalytical X’Pert MRD diffractometer for the symmetric reflection 0004 and asymmetric reflections 10–12 and  $-1-124$ .

According to the dislocation model of the tunneling current in barrier structures fabricated based on degenerate semiconductors ( $p$ – $n$  junctions, Schottky diodes,  $p$ – $n$  heterojunctions), their  $I$ – $V$  characteristics can be represented by the equation of the form [8]

$$I = I_0(\exp qV/\eta - 1), \tag{1}$$

where

$$I_0 = q\rho v_D \exp(-qV_K/\eta) \tag{2}$$

is the density of the saturation current,  $q$  is the elementary charge,  $qV_K = \phi_B - \mu_n$  is the diffusion potential for the Schottky barriers,  $\phi_B$  is the height of the Schottky barrier,  $\mu_n \cong kT \ln \frac{N_C}{N_D}$  is the chemical potential,  $N_C = 2.23 \times 10^{18} \text{ cm}^{-3}$  is the effective density of states in the conduction band of  $n$ -GaN [10],  $v_D \approx 1.5 \times 10^{13} \text{ s}^{-1}$  is

the Debye frequency for GaN,  $\rho$  is the dislocation density,  $\eta = nkT$  is the characteristic energy of tunneling,  $n$  is the ideality factor,  $k$  is the Boltzmann constant,  $T$  is the temperature, and  $N_D$  is the concentration of ionized donors in GaN equal to  $\sim 3 \times 10^{17} \text{ cm}^{-3}$  in our case.

It is evident from (2) that, knowing the values of  $I_0$ ,  $\eta$ , and  $V_K$  from the experimental  $I$ - $V$  characteristics, we can calculate the dislocation density

$$\rho = \frac{I_0(0)}{qV_D} \exp \frac{qV_K(0)}{\eta(0)}. \quad (3)$$

Here,  $I_0(0)$  and  $\eta(0)$  are obtained by extrapolation to zero of the absolute temperature of temperature dependences of  $I_0$  and  $\eta$ . According to the empirical dependence of  $\phi_B$  on the band gap  $E_g$  in GaN,  $\phi_B \approx \frac{1}{3}E_g$  let us determine the value of  $qV_K(0)$  by the formula

$$\begin{aligned} qV_K(0) &= \phi_B(0) - \mu_n(0) \cong \frac{1}{3}E_g^{\text{GaN}}(0) - \mu_n(0) \\ &\cong \frac{1}{3}E_g(0) \cong \frac{1}{3}3.47 \text{ eV} \cong 1.15 \text{ eV}, \end{aligned} \quad (4)$$

since GaN is a semiconductor material with a considerable fraction ( $\sim 50\%$ ) of ionic bonds, and the empiric dependence  $\phi_B \approx 0.6E_g$  [11], which is characteristic of either covalent semiconductors or those with a considerable fraction of the covalent bonding, is not fulfilled in our case. If we take into account that the experimental height of the Schottky barrier formed on  $n$ -GaN by pure metals (see table) Ni, Pt, Pd, Re, and Au [12, 13] is close to  $\phi_B \approx 1/3E_g$ , then  $qV_K(0)$  can be estimated by formula (4).

Almost identical values for the Schottky barriers mentioned in a table were also obtained in [14–16]. It will be shown below that the values of  $\phi_B$  of the same order of magnitude are also obtained in our experiment for the  $\text{TiB}_x$ - $n$ -GaAs Schottky barrier. However, we keep in mind that, since the fraction of the ionic strength in GaN is considerable and the density of surface states is relatively low, the Fermi level is pinned to the surface partially, which should obligatorily affect the experimental spread in the values of  $\phi_B$  for the Schottky barriers, not only fabricated both by various methods of formation but also fabricated by the same technology.

Figure 3a represents the forward portions of the  $I$ - $V$  characteristic of the Au- $\text{TiB}_x$ - $n$ -GaAs Schottky diodes measured in the temperature range 80–600 K. Figure 3b represents the temperature dependences of  $I_0$  and  $\eta$ . It is evident that, in the temperature range 80–350 K, the mechanism of charge transport is tunnel, which is indicated by a weak temperature dependence of the saturation current and absence of the temperature dependence of the characteristic energy of tunneling in this temperature range. From the  $C$ - $V$  characteristic, we calculated

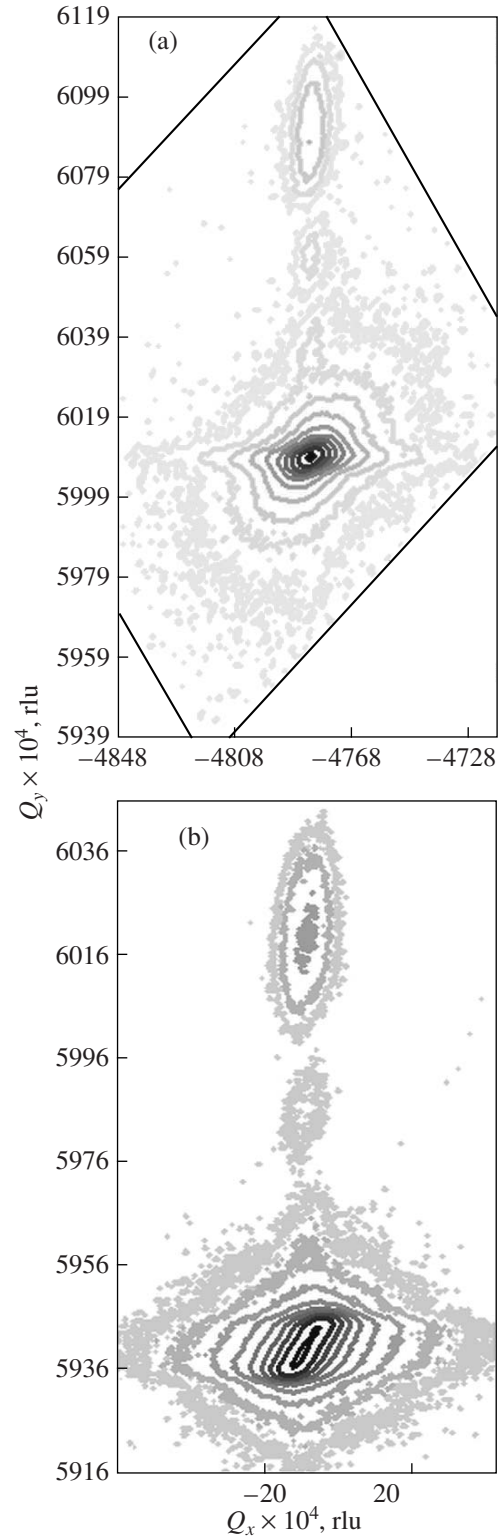


**Fig. 2.** Intensity distribution around the sites of the reciprocal lattice of (a) symmetric reflection (0004) and (b) asymmetric reflection ( $-1-124$ ) for the GaN sample grown on the  $\text{Al}_2\text{O}_3$  substrate.

the concentration of dopant, which was  $3.2 \times 10^{17} \text{ cm}^{-3}$  for the diode under study, while  $\phi_B$  calculated from the  $C$ - $V$  characteristic turned out to be equal to 1.15 eV.

Height of the Schottky barrier for GaN by the data [12, 13]

Metal	Ni	Pt	Pd	Au	Re
$\phi_B$ , eV	1.15; 1.13	1.16	1.24	1.03	1.06
Reference	[12, 13]	[13]	[13]	[12]	[13]

Taking into account  $I_0(0)$ ,  $\eta(0)$ , and  $qV_K(0)$ , the dislocation density calculated by formula (3) was equal to

$$\rho = \frac{7.35 \times 10^{-4} \text{ A/cm}^2}{1.6 \times 10^{-19} k \times 1.5 \times 10^{13} \text{ s}^{-1}} \exp\left(\frac{1.15 \text{ eV}}{0.105 \text{ eV}}\right) \approx 1.7 \times 10^7 \text{ cm}^{-2},$$

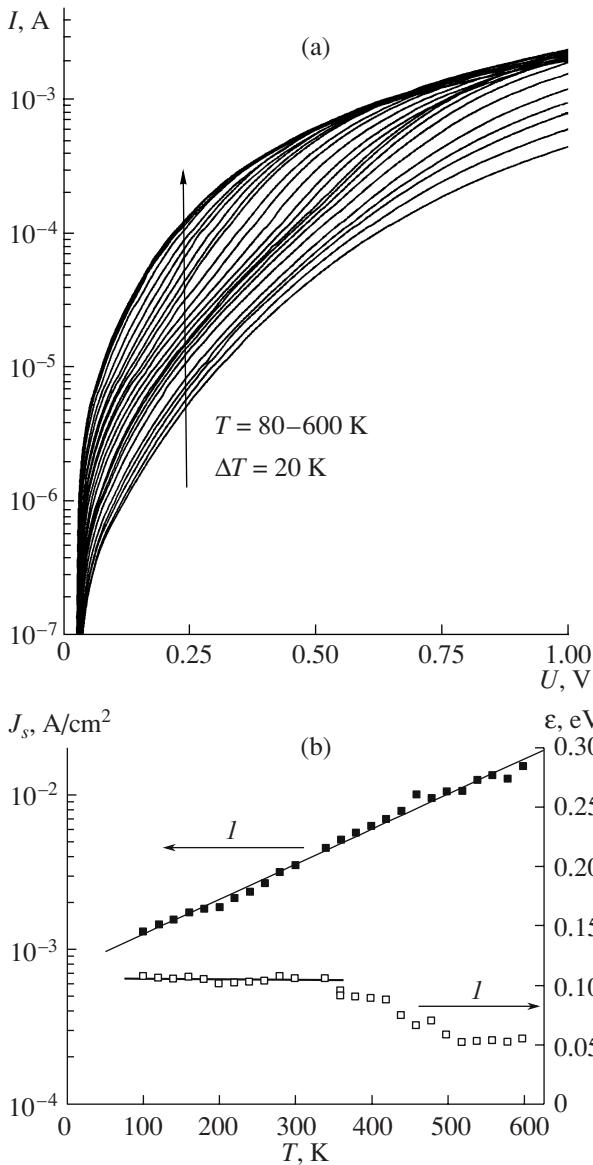


**Fig. 3.** (a) Forward portions of the  $I$ - $V$  characteristics of the Au-TiB<sub>x</sub>- $n$ -GaN Schottky diodes measured in a temperature range of 80–600 K; (b) temperature dependences (1) of the density of the saturation current and (2) of the characteristic energy of tunneling.

which is in good agreement with the results obtained from X-ray diffraction measurements. The dislocation density obtained from XRD is  $2.23 \times 10^8 \text{ cm}^{-2}$  for spreading dislocations and  $1.8 \times 10^7 \text{ cm}^{-2}$  for edge dislocations. These data agree with the results obtained in [4], where the dislocation density determined by the X-ray method in the GaN layers grown on sapphire by metal-organic vapor-phase epitaxy at ZAO Élma-Malakhit was equal to  $1-3 \times 10^8 \text{ cm}^{-2}$  for various samples. Kyutt et al. [17] give the same order of magnitudes for dislocation densities in the GaN films grown on sapphire, SiC, and GaAs. They note that irrespective of the methods and modes of epitaxy, the characteristic feature of the GaN epitaxial films is the presence of screw and edge dislocations.

Despite the possibility of describing the tunneling current using multistep tunneling, the question arises of realization of this mechanism in the Schottky barrier, the space-charge region  $W$  in which at  $N_D \approx 3 \times 10^{17} \text{ cm}^{-3}$  is much larger than the characteristic length of tunneling  $\lambda$  in GaN. Indeed, it is known that  $W$  is defined by the formula [18]

$$W \approx \left[ \frac{2\epsilon_0}{q} \left( \frac{\epsilon}{N_D} \right) (V_K - U) \right]^{1/2}, \tag{5}$$

where  $\epsilon_0$  and  $\epsilon$  are the permittivities of free space and GaN, respectively; and in our case, at  $U = 0$  and  $V_K = 1.15 \text{ V}$ ,  $W = 7 \times 10^{-5} \text{ cm}$ . Estimation of the characteristic tunneling path  $\lambda$  according to [7]

$$\lambda = \frac{\hbar}{\sqrt{2m^*q(V_K - U)}},$$

where  $\hbar$  is Planck's constant and  $m^* = 0.2m_0$  is the effective mass of the electron in GaN, gives  $\lambda \approx 0.4 \times 10^{-7} \text{ cm}$ .

A similar process was previously studied by Evstropov et al. for surface-barrier III-V-based (GaAs, GaP) structures at the ratio  $W/\lambda \approx 200-500$  for various structures [7]. An increase in the probability of tunneling [7] is associated with the tunneling charge transport along the dislocation line. Such a mechanism of charge transport can be understood if we introduce, similarly to [7], a scale factor  $r$ , which increases the characteristic tunneling path. In experiment, this circumstance manifests itself as an increase in the characteristic energy of tunneling compared, with its theoretical value  $\eta_t$ , calculated by the formula

$$\eta_t = \frac{\hbar q}{2} \left[ \frac{1}{\epsilon_0 m^*} \left( \frac{N_D}{\epsilon} \right) \right]^{1/2} \tag{6}$$

and equal to  $\sim 7 \text{ meV}$  in our case. In this case,

$$r = \frac{\eta}{\eta_t} \approx \frac{0.105 \text{ meV}}{0.007 \text{ meV}} \approx 15.$$

The charge transport in the temperature range 350–600 K is performed with prevalence of the overbarrier



current, which indicates a decrease in the value of  $\eta$  with an increase in temperature from 350 to 600 K.

#### 4. CONCLUSIONS

Thus, our experimental data indicate that the current transport in the temperature range 80–380 K in the forward-biased Au–TiB<sub>x</sub>–n–GaN Schottky barrier, despite the broad-band structure of the contact ( $W \gg \lambda$ ), proceeds by the tunneling mechanism, the nature of which is associated with dislocations emerging at the GaN/Al<sub>2</sub>O<sub>3</sub> interface during epitaxy of GaN and growing-in into the epitaxial GaN layer, which confirms the dislocation nature and a model of excess tunneling current in III–V-based degenerate barrier structures.

#### REFERENCES

1. M. S. Shur, *Solid State Electron.* **42**, 2131 (1998).
2. H. Morkos, *Nitride Semiconductors and Devices* (Springer, Berlin, 1999).
3. Yu. G. Shreter, Yu. T. Rebane, V. A. Zykov, and V. G. Sidorov, *Wide-Gap Semiconductors* (Nauka, St. Petersburg, 2001) [in Russian].
4. V. P. Klad'ko, C. V. Chornen'kii, A. V. Naumov, et al., *Fiz. Tekh. Poluprovodn.* **40**, 1087 (2006) [*Semiconductors* **40**, 1060 (2006)].
5. V. V. Evstropov, Yu. V. Zhilyaev, N. Nazarov, et al., *Fiz. Tekh. Poluprovodn.* **27**, 1319 (1993).
6. V. V. Evstropov, Yu. V. Zhilyaev, N. Nazarov, et al., *Fiz. Tekh. Poluprovodn.* **29**, 385 (1995) [*Semiconductors* **29**, 195 (1995)].
7. V. V. Evstropov, Yu. V. Zhilyaev, M. Dzhumaeva, and N. Nazarov, *Fiz. Tekh. Poluprovodn.* **31**, 152 (1997) [*Semiconductors* **31** (1997)].
8. V. V. Evstropov, M. Dzhumaeva, Yu. V. Zhilyaev, et al., *Fiz. Tekh. Poluprovodn.* **34**, 1357 (2000) [*Semiconductors* **34**, 1305 (2000)].
9. A. E. Belyaev, N. C. Boltovets, V. N. Ivanov, et al., *Pis'ma Zh. Tekh. Fiz.* **31** (24), 88 (2005) [*Tech. Phys. Lett.* **31**, 1078 (2005)].
10. *Semiconductor Materials GaN, AlN BN, SiC*, Ed. by M. E. Levinstein, S. L. Rumyantsev, and M. S. Shur (Wiley, New York, 2001).
11. M. Shur, *Physics of Semiconductor Devices* (Prentice-Hall, Englewood Cliffs, 1990; Mir, Moscow, 1992).
12. E. V. Kalinina, N. I. Kuznetsov, A. I. Babanin, et al., *Diamond Relat. Mater.* **6**, 1528 (1997).
13. J. Würfl, V. Abrosimova, J. Hilsenbeck, et al., *Microelectron. Reliab.* **39**, 1737 (1999).
14. E. Monroy, F. Calle, R. Ranchal, et al., *Semicond. Sci. Technol.* **17**, L47 (2002).
15. G. L. Chen, F. C. Chang, K. C. Shen, et al., *Appl. Phys. Lett.* **80**, 595 (2002).
16. N. Miura, T. Nanjo, M. Suita, et al., *Solid State Electron.* **48**, 689 (2004).
17. R. N. Kyutt, V. V. Ratnikov, G. N. Mosina, and M. P. Shcheglov, *Fiz. Tverd. Tela* **41**, 30 (1999) [*Phys. Solid State* **41**, 25 (1999)].
18. S. Sze, *Physics of Semiconductor Devices* (Wiley, New York, 1981; Mir, Moscow, 1984).

*Translated by N. Korovin*